A new multi-axial failure criterion for concrete

M. Como
Department of Civil Engineering, University of Rome Tor Vergata, Rome, Italy

R. Luciano
DiMSAT, University of Cassino, Cassino (Frosinone), Italy

ABSTRACT: In this paper, a new failure criterion for the concrete is developed. Cement, sand, aggregates and water are mixed together and, after the setting, the cement paste binds aggregates and hardens to form concrete. Experimentally, pores of different sizes are diffused in the hardened cement paste and micro stresses arise in the neighborhood of the small pores when the concrete is loaded. The main idea of the proposed failure criterion is based on the assumption that the macroscopic concrete failure occurs when the maximum tensile stress, around the small pores reaches the local hardened cement paste tensile strength. The proposed model explains many experimental phenomena as, for example, the different compression and tensile strengths, the different crack geometries in the tension and compression failures and the experimental failure contours under biaxial stress.

1 INRODUCTION

The research of a failure criterion for concrete under multi-axial stresses is a very important task because of its numerous civil engineering applications.
Nowadays, several concrete failure tests under multiaxial stresses are available and many theoretical failure criteria have been proposed. These criteria, on the other hand, have been formulated, as a rule, by modifying failure conditions concerning other materials, (e.g. the Coulomb criterion) to the concrete. Among all the criteria available in literature, the Rankine criterion (Van Mier, 1997, Jiràsek & Bazant, 2001, McClintock & Argon, 1966) seems to have a physical basis for the concrete. According to this criterion, in fact, concrete fails in brittle manner as soon as the maximum principal stress exceeds the concrete tensile strength. It is well known, on the other hand, that the strict application of the Rankine criterion could imply that for a compressed concrete specimen failure could never occur because no tensile stress develops. On the contrary, brittle failures are ob-served also in compressive regimes. Tensile stresses, in fact, can arise at microscopic level and produce failures. The concrete is a multiscale material consisting of aggregates embedded in a matrix of binder, the hardened cement paste (Van Mier, 1997). Further, the hardened cement paste is weakened by a capillary porosity, produced by evaporation of the water in excess. Diffused pores are visible with the electronic microscope: they have irregular shape and are spread up among the needles of calcium silicate hydrates, the structure of the hardened cement paste. When concrete is loaded, high stress concentrations take place at microscopic level around these small cavities: they produce micro cracks that propagate across the hardened cement paste till they become visible at macroscopic level.

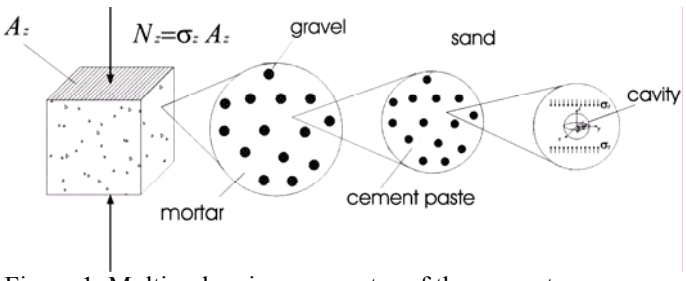

Figure 1. Multiscale micro-geometry of the concrete.

Many contributions are available in literature which use Micromechanics to estimate the mechanical properties of the concrete e.g. the elastic moduli (Yang & Huang, 1996). In line with this approach, ere, two steps homogenization technique is used to evaluate the stresses supported by the cement paste when the concrete is loaded (Fig.1). In the first step, the global moduli of the mortar are evaluated. In the second step these moduli are used to estimate the behaviour of the concrete made by the mortar and the gravel. Combining these two results, obtained at two different scales, we can evaluate the average stresses in the hardened cement paste. These mean stresses represent the asymptotic stress state for the

local stresses acting around the small pores diffused in the hardened cement paste. These local stresses are responsible of the failure in the concrete: at microscopic level collapse occurs when the maximum tensile stress around the pores reaches the tensile strength of the hardened cement paste.

In the above exposed framework a biaxial failure contour is analytically obtained for concrete. The comparison of this theoretical criterion with several experimental results seems to be satisfying.

2 2 STRESS CONCENTRATIONS AROUND THE PORES DIFFUSED IN THE HARDENED CEMENT PASTE

Concrete can be considered a material homogeneous and isotropic at average level. Mean stresses in the various components can be obtained by using the so called mixtures law and the elasticity equations. (Nemat-Nasser & Hori, 1999). In this formulation strong simplifications can be obtained by assuming the same average Poisson ratios for the components of the concrete, as approximately it does occur. In this case, as stated beforehand, we consider a two steps homogenization procedure: in the first step, the mortar is made by sand and hardened cement paste while, in the second step, the concrete is composed by mortar and gravel. Thus we get:

$$\sigma_x^p = K_2\sigma_x^c; \quad \sigma_y^p = K_2\sigma_y^c; \quad \sigma_z^p = K_2\sigma_z^c \tag{1}$$

where:

$$K_2 = K_2^{p,m}K_2^{m,c} \tag{2}$$

$$K_2^{p,m} = \frac{E_p}{E_m}\frac{(1-\bar{\nu}-2\bar{\nu}^2)}{1-\rho_s}\frac{E_s^2 - E_mE_s - E_sE_p + E_mE_p}{D} \tag{2a}$$

$$K_2^{m,c} = \frac{E_m}{E_c}\frac{(1-\bar{\nu}-2\bar{\nu}^2)}{1-\rho_g}\frac{E_g^2 - E_cE_g - E_gE_m + E_cE_m)}{D} \tag{2b}$$

with:

$$D = E_m^2(1-\bar{\nu}-2\bar{\nu}^2) - E_gE_m(2-2\bar{\nu}-4\bar{\nu}^2) + E_g^2(1-\bar{\nu}-2\bar{\nu}^2) \tag{2c}$$

where E is the Young modulus and the indices c, g, m, s, p indicate concrete, gravel, mortar, sand and cement paste respectively. The elastic moduli of the constituents and of the concrete are related; in fact the elastic modulus of the mortar must be the result of an homogenization process in which the constituents are the sand and the cement paste. In the same way, the elastic modulus of the concrete is obtained from the homogenization of mortar and gravel. Therefore E_c and E_m can be obtained by using a micromechanical models and must satisfy the Hashin-Shtrikman bounds which depend on the geometry and the volume fraction of the constituents (Nemat-Nasser & Hori, 1999). If such a constraint is not satisfied, i.e. E_c and E_m are chosen arbitrarily, the results obtained by using the proposed failure model can be physically uncorrected since the elastic moduli are meaningless. Therefore in eqs. (3a) and (3b), concrete and mortar moduli will be suitably chosen by using micromechanics and accurate test results in order to effectively represent the elasticity of the composite materials. Strong stress concentration occurs around the small cavities spread up inside the hardened cement paste. In order to define these local stresses can be assumed that the mean stress inside the hardened cement paste is the asymptotic stress acting at large distance from the single pore. Thus, when the concrete is, for instance, axially loaded by the uniform stresses σ_z, and the mean stress σ_z^P takes place inside the hardened cement paste, by assuming for the pore a spherical shape, the local stress around the cavity is (McClintock & Argon, 1966):
at the pole P_z (see Fig.2):

$$\begin{aligned} &\sigma_{RR}^{P_z} = 0 \\ &\sigma_{\vartheta\vartheta}^{P_z} = \sigma_{\varphi\varphi}^{P_z} = A(\nu)\cdot\sigma_z^p \end{aligned} \tag{3a}$$

at the equator E_z:

$$\sigma_R^{E_z} = 0; \quad \sigma_{\varphi\varphi}^{E_z} = B(\nu)\cdot\sigma_z^p; \quad \sigma_{\vartheta\vartheta}^{E_z} = C(\nu)\cdot\sigma_z^p \tag{3b}$$

$A(\nu)$, $B(\nu)$, $C(\nu)$ depend on the Poisson ratio ν of the hardened cement paste and are given by:

$$\begin{aligned} &A(\nu) = -\frac{3+15\nu}{2\cdot(7-5\nu)}, \; B(\nu) = \frac{27-15\nu}{2\cdot(7-5\nu)}, \\ &C(\nu) = -\frac{3-15\nu}{2\cdot(7-5\nu)} \end{aligned} \tag{4}$$

where ν indicates the local Poisson ratio of the hardened cement paste without pores, larger than the average Poisson ratio $\bar{\nu}$.

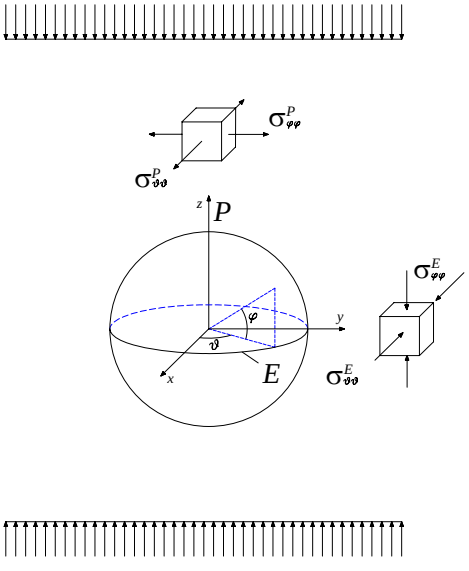

Figure 2. Local stress around the spherical pore under an asymptotic compressive stress.

Actually, the small pores spread up in the hardened cement paste have irregular shape. Pores of irregular shape in plane elasticity can be represented by small elliptic holes having various orientation. High stress concentrations occur on the boundaries of elliptic cavities with the major axis orthogonal to the direction of the applied uniaxial tensile stress. The stress component $\sigma_{y,}$ acting at the end of the major axis, increases strongly while the other ones hold almost the same (Fig.3).

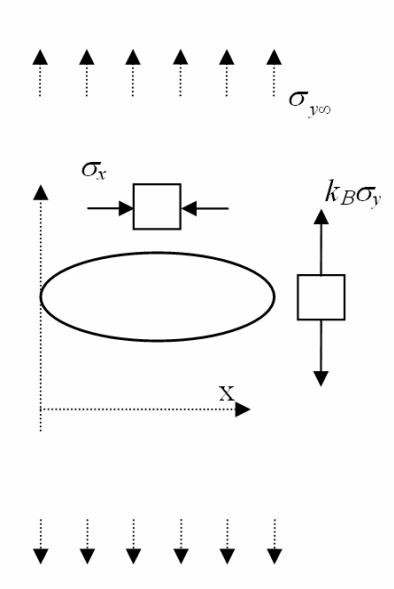

Figure 3 Stress concentrations around an elliptic cavity

At the end of the minor axis the circumferential stress σ_x changes sign but its intensity almost does not increase. Thus, taking into account the irregular shape of the pores diffused in the hardened cement paste, we assume that the long ellipsoids pores with the major axis orthogonal to the applied tensile stress, will exhibit the highest stress concentration and will be the first to fail. To the authors' knowledge, there is no simple analytical solution able to describe the local stress field in the neighbourhood of an ellipsoidal cavity. Thus, for sake of simplicity, we continue to use the field equations describing stresses occurring along the boundary of the spherical pore but increasing the intensity of the stress component directed as the applied tension. Thus, introducing the intensity factor k_B to take into account the irregular shape of the cavity, we modify the expression of the local stress field (3a) and (3b) concerning the spherical hole in the following way:
at the pole P_z:

$$\sigma_{RR}^{P_z} = 0$$
$$\sigma_{\vartheta\vartheta}^{P_z} = \sigma_{\varphi\varphi}^{P_z} = A(\nu)\cdot\sigma_z^P \qquad (3a')$$

but, at the equator E_z:

$$\sigma_R^{E_z} = 0; \quad \sigma_{\varphi\varphi}^{E_z} = k_B B(\nu)\cdot\sigma_z^P; \quad \sigma_{\vartheta\vartheta}^{E_z} = C(\nu)\cdot\sigma_z^P \qquad (3b')$$

3 THE FAILURE CONDITION

Failure occurs when the maximum principal tensile stress around the capillary pores of the hardened cement paste reaches its tensile strength. This condition, even if of local character, concerns all the cavities continuously diffused in the hardened cement paste and, when reached, produces the macroscopic destruction of the binder and, accordingly, the concrete failure.

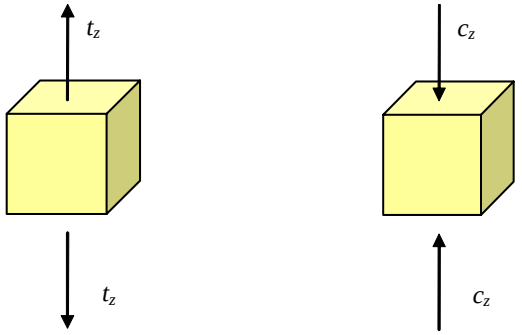

Figure 4 Uniaxial tension and uniaxial compression

Under increasing tensile stress acting on the concrete, $\sigma_{\varphi\varphi}^{E_z}$, acting at the poles P_y and P_x, i.e. along the equatorial circle E_z of the cavities, can reach the tensile strength of the hardened paste and produce failure. Cracks are thus orthogonal to the $\sigma_{\varphi\varphi}^{E_z}$, i.e. orthogonal to the applied tensile stress. Concrete in uniaxial tension thus fails when

$$f_{rt,loc}^{p} = \sigma_{\varphi\varphi}^{E_z} = k_B B(\nu) K_2 f_{rt}^{c} \qquad (5)$$

where $f_{rt,loc}^{p}$ and f_{rt}^{c} indicate the tensile strengths of the hardened cement paste and concrete respectively. Conversely, in presence of uniform compression $\sigma_{z,}$ the tensile strength of the cement paste is reached at poles P_z of the of the cavities. In this case the failure condition is:

$$f_{rt,loc}^{p} = -A(\nu)\cdot K_2 f_{rc.un}^{c} \qquad (6)$$

Cracks will now be parallel to the compression stress σ_z acting on the concrete.

By tests, in the case of uniform uniaxial compression, cracks turn out parallel to the direction of the applied compression while, in the case of uniaxial tension, cracks are orthogonal to the applied tensile stress. These results are captured by the present model of concrete failure because it takes into account the different local failures occurring at the pole or at the equator of the pores diffused in the cement paste.

At the same value of the stress acting on the concrete, the maximum local tensile stress, produced in the binder when the concrete is in uniaxial compression, is much lower than the maximum local tensile stress occurring when the concrete is in uniaxial tension. Thus, the intensity of the stress applied to the

concrete, able to produce compression failure, will be much higher than the stress intensity required to produce tensile failure. The proposed failure model is therefore able to explain why the tensile concrete strength is much lower than the compression one.

In order to validate the proposed concrete failure model, on the other hand, it is required that the maximum local tensile stress, corresponding to the concrete compression failure, is equal to the maximum local tensile stress occurring in the concrete in uniaxial tension. Thus we have the condition

$$-A(\nu)\cdot K_2 f^c_{rc.un} = k_B B(\nu) K_2 f^c_{rt} \tag{7}$$

and:

$$k_B = -\frac{A(\nu)}{B(\nu)}\frac{f^c_{rc.un}}{f^c_{rt}} \tag{8}$$

For normal strength concrete (*NC*), the uniform compression strength $f^c_{rc.un}$ is lower than the standard cylindrical compression strength and we can write

$$f^c_{rc.un} = \gamma f^c_{rc} \tag{9}$$

where γ depends on the used restraint at the specimen boundary (Van Mier, 1997) and can be assumed equal to *0,85÷0,90*. Further, the tensile concrete strength f^c_{rt} can be evaluated in terms of the cylindrical compression strength f^c_{rc} with:

$$f^c_{rt} = \beta f^c_{rc} \tag{10}$$

where the constant β is about *0,10* (Van Mier, 1997). Thus we get

$$f^c_{rt} = f^c_{rc.un}\beta/\gamma \tag{11}$$

with $f^c_{rc.un} / f^c_{rt} \approx 8 \div 9$ and

$$k_B = -\frac{A(\nu)}{B(\nu)}\frac{\gamma}{\beta} \tag{12}$$

Taking into account the range of values of the β and γ the concentration factor k_B is about 2,5.

We can also obtain the local tensile strength of the hardened cement paste, in fact

$$f^p_{rt,loc} = k_B B(\nu) K_2 f^c_{rt} \tag{13}$$

and we get, by assuming for the value of the local Poisson ratio of the hardened cement paste $\nu = 0{,}25$,

$$f^p_{rt,loc} \approx 3{,}75 f^c_{rt} \tag{13'}$$

The local strength of the hardened cement paste, i.e. the tensile strength of the binder not weakened by the diffused porosity, is much higher than the tensile concrete strength.

4 BIAXIAL FAILURE CONTOUR FOR THE CONCRETE

Biaxial stress states are very frequent. The biaxial stress regimes are of four different kinds: 1. compression-compression (*Bcc*) 2. compression-traction (*Bct*), 3, traction-compression (*Btc*) 4. traction-traction (*Btt*). We will examine the corresponding possible concrete failures.

4.1 *Compression - compression (Bcc)*

The uniform vertical compression σ_z is applied on the concrete perpendicular to the horizontal compression σ_y (Fig.5).

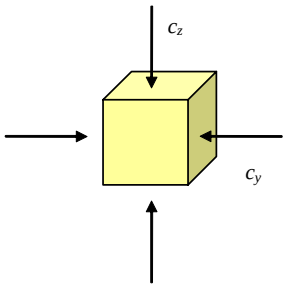

Figure 5. The compression – compression regime

If c_z e and c_y are compressions, then

$$\sigma_y = -c_y \quad \sigma_z = -c_z \tag{14}$$

with $c_z \geq c_y$. The asymptotic stresses acting at large distance from the pore in the hardened cement paste are:

$$\sigma_{z\infty} = -c_z K_2 \quad \sigma_{y\infty} = -c_y K_2 \quad \sigma_{x\infty} = 0 \tag{14'}$$

to which correspond the local stresses:

$$\begin{aligned}
\sigma^{P_z}_{\phi\phi} &= [-A(\nu)c_z - k_B B(\nu)c_y]K_2 \\
\sigma^{P_z}_{\theta\theta} &= [-A(\nu)c_z - C(\nu)c_y]K_2 \\
\\
\sigma^{P_y}_{\phi\phi} &= [-k_B B(\nu)c_z - A(\nu)c_y]K_2 \\
\sigma^{P_y}_{\theta\theta} &= [-C(\nu)c_z - A(\nu)c_y]K_2 \\
\\
\sigma^{P_x}_{\phi\phi} &= [-k_B B(\nu)c_z - C(\nu)c_y]K_2 \\
\sigma^{P_x}_{\theta\theta} &= [-C(\nu)c_z - k_B B(\nu)c_y]K_2
\end{aligned} \tag{15}$$

Taking into account the sign of the quantities $A(\nu)$, $B(\nu)$ e $C(\nu)$, the higher tensile stress is reached by the $\sigma^{P_z}_{\vartheta\vartheta}$ at the pole P_z of the pore. On the contrary, with c_y dominating, the higher tensile stress is produced by the $\sigma^{P_y}_{\vartheta\vartheta}$ at the pole P_y (Fig.6). The failure condition will be attained when firstly one of the following conditions, linear in c_y and c_z is satisfied:

$$\sigma^{P_z}_{\vartheta\vartheta} = [-A(\nu)c_z - C(\nu)c_y]K_2 = f^{p}_{rt,loc},\ c_z \geq c_y \qquad (16)$$

$$\sigma^{P_y}_{\vartheta\vartheta} = [-A(\nu)c_y - C(\nu)c_z]K_2 = f^{p}_{rt,loc},\ c_y \geq c_z \qquad (16')$$

or:

$$c_z + \frac{C(\nu)}{A(\nu)}c_y = f^{c}_{rc,un} \qquad c_y + \frac{C(\nu)}{A(\nu)}c_z = f_{rc,un} \qquad (17)$$

according to $c_z \geq c_y$ or $c_y \geq c_z$.

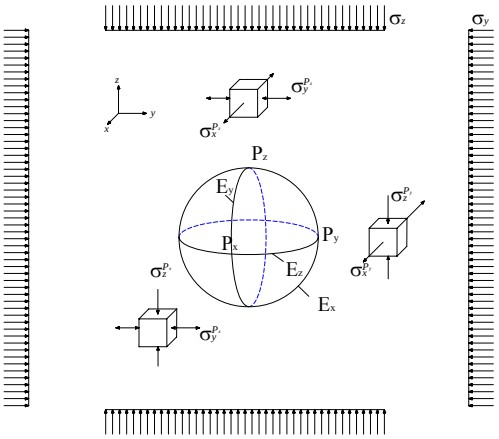

Figure 6. Local stresses around the pores in the Bcc regime

In Figure 12 the half lines AK and BK are the failure contours corresponding to eqs.(16) e (16'). As a rule, $A(\nu)<0$ e $C(\nu)>0$ when $\nu>0{,}20$. Thus, the biaxial concrete compression strength is larger than the uniaxial strength. Particularly, when:

$$c_y = c_z = c_{biass} \qquad (18)$$

we have the concrete strength under equi-biaxial compressions

$$c_{biass} = f^{c}_{rc,un.biass} \qquad (19)$$

with:

$$f^{c}_{rc,un.biass} = \frac{f^{c}_{rc,un}}{1 + C(\nu)/A(\nu)} \qquad (20)$$

For instance, with ν = 0,25, eq. (20) gives:

$$f^{c}_{rc,un.biass} = 1{,}125\, f^{c}_{rc,un}$$

4.2 *Compression-tension (Bct) e tension-compression(Btc)*

In this case, the uniform vertical compression σ_z is applied on the concrete perpendicular to the horizontal tensile stress σ_y (Fig.7) and we have

$$\sigma_z = -c_z \quad \sigma_y = t_y \qquad (21)$$

where c_z and t_y are the intensities of the applied stresses.

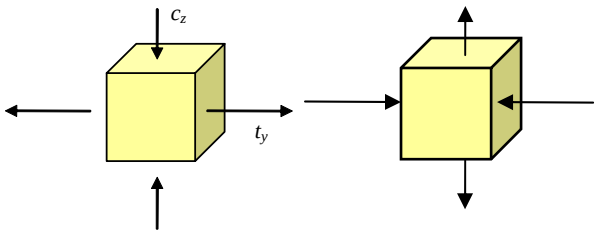

Figure 7. The (Bct) and the (Btc) regimes

At the poles of the cavities diffused in the hardened cement paste we have the stresses

$$\sigma^{P_z}_{\phi\phi} = K_2[-A(\nu)c_z + k_B B(\nu)t_y]$$
$$\sigma^{P_z}_{\theta\theta} = K_2[-A(\nu)c_z + C(\nu)t_y]$$

$$\sigma^{P_y}_{\phi\phi} = K_2[-k_B B(\nu)c_z + A(\nu)t_y]$$
$$\sigma^{P_y}_{\theta\theta} = K_2[-C(\nu)c_z + A(\nu)t_y] \qquad (22)$$

$$\sigma^{P_x}_{\phi\phi} = K_2[-k_B B(\nu)c_z + C(\nu)t_y]$$
$$\sigma^{P_x}_{\theta\theta} = K_2[-C(\nu)c_z + k_B B(\nu)t_y]$$

Thus, with c_z dominating and taking into account the values of the coefficients $A(\nu)$, $B(\nu)$ e $C(\nu)$, the higher local tensile stress is reached at the pole P_z by the component $\sigma^{P_z}_{\phi\phi}$.(Fig.8). Thus the failure condition is now:

$$-A(\nu)c_z + k_B B(\nu)t_y = f^{p}_{rt,loc}/K_2 \qquad (23)$$

or

$$c_z = f^{c}_{rc.un} - \frac{f^{c}_{rc.un}}{f^{c}_{rt}}t_y \qquad (24)$$

represented in Figure 12 by the straight line *BP*.

Analogously, in the case of traction – compression, we have

$$c_y = f^{c}_{rc.un} - \frac{f^{c}_{rc.un}}{f^{c}_{rt}}t_z \qquad (24')$$

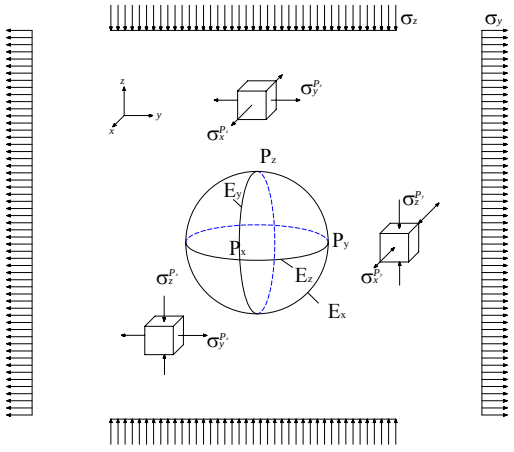

Figure 8. Local stresses around the pores in the (Bct)/(Btc) regimes

The straight lines BP and *AQ* of Figure 12 represent the failure conditions (24) and (24') for the compression- tension and tension- compression regimes. Thus, when a small lateral tensile component is applied, the strength decreases significantly in the compressive direction. When the two stresses with opposite sign have the same intensity, as it occurs in the case of *pure shear* (Fig.9),

$$\sigma_z = -\tau_{or} \quad \sigma_y = \tau_{or} \tag{25}$$

the failure shear stress is:

$$\tau_{or} = \frac{f_{rt,un}}{1 + f_{rt,un} / f_{rc,un}} \tag{26}$$

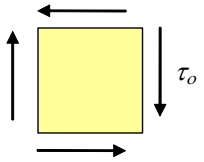

Figure 9. The pure shear regime

4.3 *Traction - traction(Btt)*

The mean stresses acting on the concrete are the tensile stresses (Fig.10)

$$\sigma_z = t_z \qquad \sigma_y = t_y \tag{27}$$

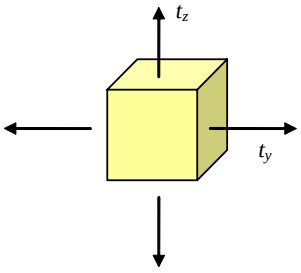

Figure 10. The tension – tension regime

Consequently, the mean stresses acting on the hardened cement paste are

$$\sigma_{z\infty} = t_z K_2 \quad \sigma_{y\infty} = t_y K_2 \tag{28}$$

and the local stresses around the pores are

$$\sigma_{\phi\phi}^{P_z} = [A(\nu)t_z + k_B B(\nu)t_y]K_2$$

$$\sigma_{\theta\theta}^{P_z} = [A(\nu)t_z + C(\nu)t_y]K_2$$

$$\sigma_{\phi\phi}^{P_y} = [k_B B(\nu)t_z + A(\nu)t_y]K_2$$

$$\sigma_{\theta\theta}^{P_y} = [C(\nu)t_z + A(\nu)t_y]K_2 \tag{29}$$

$$\sigma_{\phi\phi}^{P_x} = [k_B B(\nu)t_z + C(\nu)t_y]K_2$$

$$\sigma_{\theta\theta}^{P_x} = [C(\nu)t_z + k_B B(\nu)t_y]K_2$$

with t_z dominating on t_z, the higher tensile stress is reached by the component $\sigma_{\phi\phi}^{P_x}$ and occurs at the pole P_x (Fig.11). The failure condition thus is

$$k_B B(\nu)t_z + C(\nu)t_y = f_{rt,loc}^{p} / K_2 \tag{30}$$

or,

$$C(\nu)t_z + k_B B(\nu)t_y = f_{rt,loc}^{p} / K_2 \tag{30'}$$

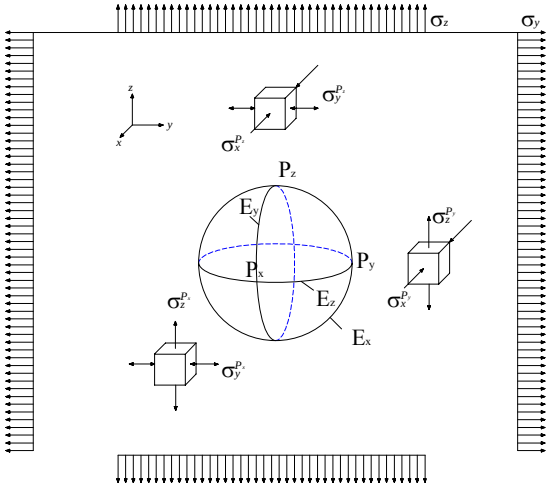

Figure 11 Local stresses around the pores in the (Btt) regime

Eqs. (30) and (30') , more clearly, become

$$t_z + \frac{C(\nu)}{k_B B(\nu)} t_y = f_{rt}^{c} \tag{31}$$

$$t_y + \frac{C(\nu)}{k_B B(\nu)} t_z = f_{rt}^{c} \tag{31'}$$

It is relevant the case of the uniform equi-biaxial tensile stress:

$$t_z = t_y = t_{biass} \tag{32}$$

Thus we get:

$$t_{biass} = \frac{f_{rt}^{c}}{1 + \frac{C(\nu)}{k_B B(\nu)}} \tag{33}$$

Eqs. (31) e (31') respectively correspond to the segments QW e PW of Figure 12.

Thus the equi-biaxial tensile strength has to be lower than the uniaxial tensile strength. Each of the failure conditions (31), (31'), (24), (24'), (17), concerning the different stress regimes of the concrete, is linear in the components σ_y, σ_z and define convex sub-regions in the σ_y, σ_z plane. The intersections of all these convex regions define the convex safe region in the biaxial stress components σ_y, σ_z whose boundary is the biaxial failure contour of the concrete (Fig.12).

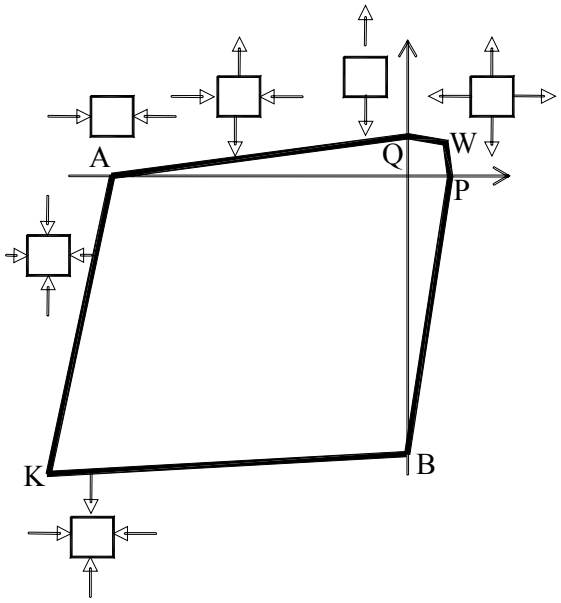

Figure 12. The obtained concrete biaxial failure contour

5 CONCLUSIONS

Figure 13 gives the biaxial failure contour for a concrete obtained experimentally by (Kupfer, 1973). Other failure contours have similar behaviour (Van Mier, 1997). It is immediate to recognize the essential good agreement of these test results with the contours corresponding to the proposed failure model of the concrete. In the compression – compression regime, when the ratio between the two principal stresses is about 0.5, the agreement is less satisfying since in this case the test results seem to be strongly influenced by the restraints used at the specimen boundary, as shown in Figure 3.84 of (Van Mier, 1997).

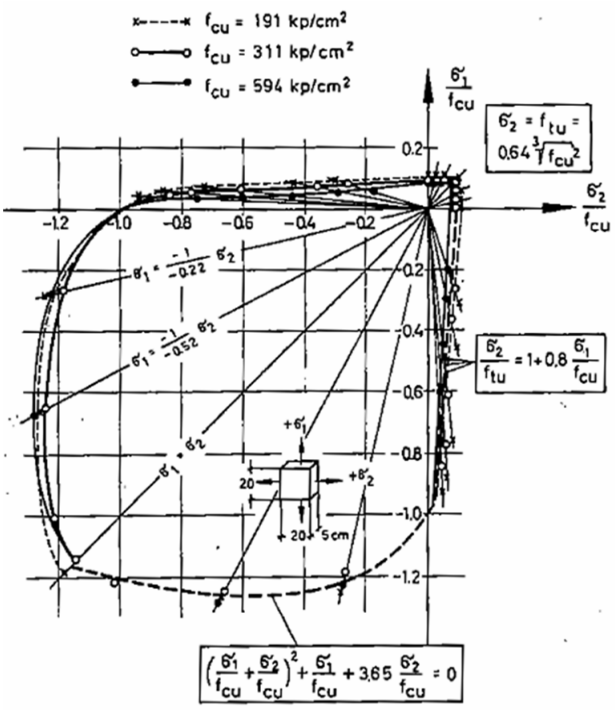

Figure 13. Failure surface of the concrete in biaxial stress conditions obtained by (Kupfer, 1973)

REFERENCES

Van Mier, JGM. 1997. Fracture processes of concrete, CRC Press, Boca Raton.

Jiràsek M, Bazant ZP. 2001. Inelastic Analysis of structures, John Wiley, New York.

McClintock FA, Argon AS. 1966. Mechanical Behaviour of materials, *Addison Wesley Publishing Company*, inc Reading, Massachusetts.

Yang CC, Huang R. 1996. Double Inclusion Model for Approximate Elastic Moduli of Concrete Material, *Cement and Concrete Research*, 26(1): 83-91.

Nemat-Nasser S, Hori M. 1999. Micromechanics: overall properties of heterogeneous materials, Elsevier, Amsterdam.

Kupfer, H. 1973. Behaviour of concrete under multiaxial short term loading, with emphasis on biaxial loading, *Deutscher Ausschuss fur Stahlbeton*, Vol.254, Berlin (in German)